NANO LETTERS

LETTER

pubs.acs.org/NanoLett

Real-Space Mapping of Fano Interference in Plasmonic Metamolecules

Pablo Alonso-Gonzalez,[†] Martin Schnell,[†] Paulo Sarriugarte,[†] Heidar Sobhani,[‡] Chihhui Wu,[§] Nihal Arju,[§] Alexander Khanikaev,[§] Federico Golmar,[∥,⊥] Pablo Albella,[#,†] Libe Arzubiaga,[∥] Felix Casanova,[∥,▽] Luis E. Hueso,[∥,▽] Peter Nordlander,[*,‡] Gennady Shvets,[*,§] and Rainer Hillenbrand[*,†,▽]

[†]Nanooptics Group, CIC nanoGUNE Consolider, 20018 Donostia-San Sebastian, Spain

[‡]Department of Physics, Rice University, MS 61, Houston, Texas 77005, United States

[§]Department of Physics, The University of Texas at Austin, One University Station C1600, Austin, Texas 78712, United States

[∥]Nanodevices Group, CIC nanoGUNE Consolider, 20018 Donostia-San Sebastian, Spain

[⊥]I.N.T.I.—CONICET, Av. Gral. Paz 5445, Ed. 42, B1650JKA, San Martín, Bs As, Argentina

[#]Centro de Física de Materiales CSIC-UPV/EHU and DIPC, Paseo Manuel de Lardizabal 4, 20018, Donostia-San Sebastian Spain

[▽]IKERBASQUE, Basque Foundation for Science, 48011 Bilbao, Spain

Supporting Information

ABSTRACT: An unprecedented control of the spectral response of plasmonic nanoantennas has recently been achieved by designing structures that exhibit Fano resonances. This new insight is paving the way for a variety of applications, such as biochemical sensing and surface-enhanced Raman spectroscopy. Here we use scattering-type near-field optical microscopy to map the spatial field distribution of Fano modes in infrared plasmonic systems. We observe in real space the interference of narrow (dark) and broad (bright) plasmonic resonances, yielding intensity and phase *toggling* between different portions of the plasmonic metamolecules when either their geometric sizes or the illumination wavelength is varied.

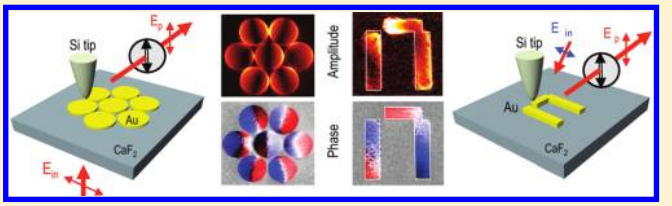

KEYWORDS: Fano resonance, scanning near-field optical microscopy, plasmon, near-field coupling, metamaterials, near-field spectroscopy

The ability to assemble subwavelength plasmonic nanoparticles and antennas[1−3] into controlled geometrical structures is revolutionizing our ability to control and manipulate light across the entire electromagnetic spectrum.[4−8] The optical properties of a nanoparticle aggregate are determined by its symmetry and the interparticle spacings, just like the electronic properties of a molecule depend on its constituent molecules and interatomic separations.[9] Highly exotic optical properties of such assemblies, often referred to as metamolecules[10,11] or metamaterials, have been observed during the past decade, including ones that have never been seen in nature, such as materials with negative refractive index and indefinite permittivity.[12,13] Using plasmonic nanostructures, it has also become possible to emulate some of the unusual optical phenomena whose origin was thought to be of quantum-mechanical nature, such as the electromagnetically induced transparency (EIT),[14−17] slow light,[18] and Fano interferences.[19−26] The advantage of using tunable plasmonic nanostructures in this context is that all these phenomena can be extended well beyond the spectral region where they were originally observed in atomic/molecular systems, giving rise to a variety of exciting applications.

Many of these applications, such as linear and nonlinear spectroscopy,[27,28] rely on the ultrasharp resonances (and related very large electric field enhancements) that have been observed in the plasmonic nanostructures exhibiting non-Lorentzian spectral extinction lines, also known as Fano resonances. The physical origin of the Fano resonances is the interference between two electromagnetic eigenmodes of the nanostructure, often referred to as "bright" and "dark", that possess strongly differing radiative lifetimes: short for the bright and long for the dark modes, respectively. When both resonances are excited by the incident electromagnetic field, they contribute to the reflected field according to their dipole strength and lifetimes and, depending on the wavelength, exhibit either constructive or destructive interference in the far field.

Up to now, the interpretation of the constructive and destructive Fano interferences has been based on far-field spectroscopy and calculations of the charge density distributions.[24,25,29] Such characterization of multiresonant metamolecules is both insufficient and ambiguous because the same far-field scattering pattern can be caused by different charge distributions. For example, while destructive interference—yielding a dip in the extinction spectrum—can be directly measured in the far field, its root cause (charge redistribution between different portions of the plasmonic meta-molecules) cannot be experimentally confirmed.

Received: June 24, 2011
Revised: August 15, 2011
Published: August 19, 2011

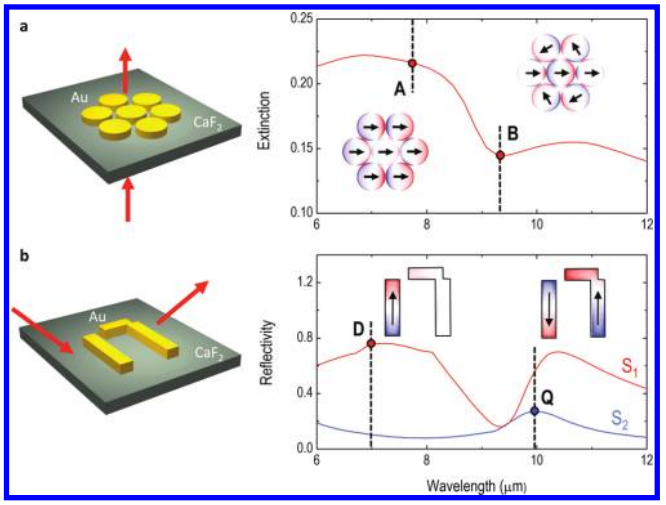

Figure 1. Fano interference in mid-infrared plasmonic metamolecules. (a) Numerically calculated extinction spectrum (right) of a heptamer structure consisting of seven gold disks (left). The insets display the charge density distribution of the superradiant mode (A) and in the Fano minimum (B). (b) Numerically calculated reflection spectrum (right) of an asymmetric PI structure (left). The insets display the charge density distribution of the dipole mode (D) and the quadrupole mode (Q). The red curve displays the reflection spectrum for s-polarized incidence with polarization parallel to the long rods. The blue curve displays the reflection spectrum for s-polarized incidence with polarization parallel to the short rod.

In this Letter, we use interferometric scattering-type scanning near-field optical microscopy (s-SNOM)[30−34] to experimentally verify the theoretically predicted near-field patterns in Fano-resonant metamolecules. We present near-field optical amplitude and phase images of highly symmetric heptamer structures[25] comprised of plasmonic disks (shown in Figure 1a) and an asymmetric PI-shaped arrangement of plasmonic nanorod antennas (Figure 1b), which were both fabricated using top-down electron beam lithography. What conceptually unites these two structures is that they both support a "dark" and a "bright" resonance, which can interfere with each other producing Fano resonances in the extinction and reflection spectra. We can change the relative phase of these interfering resonances in two complementary ways: by tuning the laser frequency (as done for the PI structures) and by changing the sizes of the plasmonic molecules (as done for the heptamers structures). Our near-field optical measurements directly demonstrate that, for both approaches, Fano interferences result in the phenomenon of *intensity toggling*: strong spatial redistribution of the high-field areas inside the metamolecules upon crossing the "dark" resonance. To date, no direct experimental evidence of interfering electromagnetic eigenmodes of plasmonic metamolecules (or their arrays constituting a metamaterial) has been presented.

In Figure 1a we illustrate a typical Fano resonance in a heptamer structure consisting of seven gold disks of 2.70 μm in diameter on a CaF_2 substrate. Calculating the extinction spectrum of this structure, we find a resonance in the mid-infrared spectral range at about 8 μm wavelength, accompanied by a minimum at around 9.3 μm. A similar spectral behavior has been previously observed for heptamer resonances at higher frequencies,[25,29] which have been fabricated using both bottom-up[25] and top-down[29] approaches. The calculated charge density plot at about 8 μm wavelength (position A in Figure 1a) shows the surface charge density on each disk, as well as the individual electric dipole moments (black arrows), which are all oriented in the same direction. Thus, the predominantly excited eigenmode is the bright one, resulting in strong scattering and extinction (bright mode). The Fano minimum in the extinction spectrum at λ = 9.3 μm (position B in Figure 1a) can be explained by the suppression of scattering caused by the destructive Fano interference between the bright and dark plasmonic eigenmodes, which minimizes the total dipole moment of the heptamer structure.

Fano resonances can also be directly observed in reflection geometry, which is illustrated with an asymmetric PI structure in Figure 1b. The calculated reflection spectrum (S_1, vertical light polarization along the long rods) exhibits two peaks and one dip. The isolated broad peak around λ = 7.1 μm is caused by the "bright" dipolar resonance (D), as clearly seen in the charge density plot. The closely spaced dip (at λ = 9.3 μm) and the second peak (at λ = 10.3 μm) are associated, respectively, with the destructive and constructive Fano interferences between the "bright" dipolar (D) and "dark" quadrupolar (Q) resonances. The actual spectral position of the Q mode (which can only be inferred to be between the dip and the second peak in the S_1 spectrum) can be determined from the reflection spectrum S_2 for horizontal light polarization along the short rod. A unique characteristic of the nonsymmetric PI-shaped plasmonic structure is that it provides us with an opportunity to precisely isolate the spectral position and lifetime of the "dark" mode using orthogonally polarized spectroscopy.

Figure 2a illustrates the experiment with the heptamer structures. We use a transmission-mode s-SNOM,[30,31] where plane wave illumination from below the sample surface is employed. Near-field amplitude $|E_z|$ and phase φ_z imaging is performed by detecting the light scattered from the scanning probe tip with a pseudoheterodyne interferometer,[35] simultaneously to topography (gray image in Figure 2a). We perform the experiments at a fixed incident wavelength of λ = 9.3 μm because of the limited wavelength range of the present setup. In order to observe the intensity *toggling* due to Fano interference that occurs upon crossing the "dark" resonance, we imaged heptamer structures of different sizes. As seen in the calculated extinction spectra (Figure 2b), the Fano minimum shifts to smaller wavelengths when the radius R of the disks is reduced. We image the bright or superradiant mode for R = 1.80 μm and for R = 1.15 μm, and the Fano interference for R = 1.35 μm. For the heptamers with R = 1.80 μm and R = 1.15 μm disks, we find a typical dipole pattern on each disk.[25] Each dipole is oriented in the same direction, oscillating with nearly the same phase, such that a strong total dipole moment is generated. For the R = 1.35 μm disks, the amplitude distribution is similar; however, the patterns on the upper and lower disks are rotated in both experiment and theory. The most significant change is observed in the phase image. The central disk still exhibits a dipolar pattern, but the fields oscillate about 90° out of phase with the outer disks, thus reducing the total dipole moment of the heptamer structure. Comparing the experimental results (Figure 2d) with the numerical calculations (Figure 2c), we find excellent agreement. A dramatic intensity and phase *toggling* from the outer-ring disks to the central disk is clearly observed in the experiment.

An interesting observation is made when comparing the real part of the charge density distribution of the heptamer structure at the Fano dip (position B in Figure 1a) with the corresponding amplitude and phase near-field images (Figure 2b, R = 1.35 μm). In the charge density plot, the entire center row seems to be 180° out of phase with the upper and lower disks. However, the near-field

dx.doi.org/10.1021/nl2021366 |*Nano Lett.* 2011, 11, 3922–3926

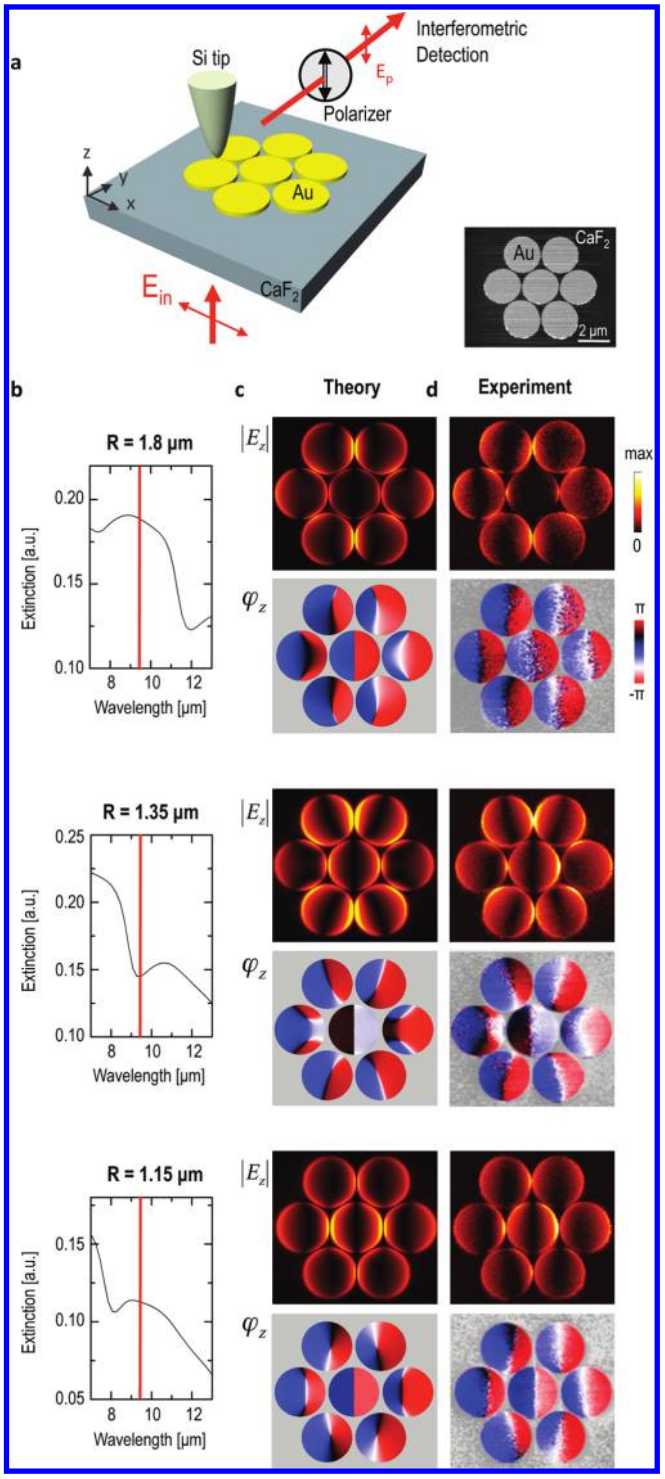

Figure 2. Real-space mapping of Fano interference in symmetric heptamer structures. (a) Experimental setup for near-field imaging in transmission mode. The heptamer structure is illuminated from below. Near-field imaging is performed by recording the tip-scattered radiation with an interferometer, yielding amplitude and phase images simultaneously to topography (gray image to the right). (b) Calculated far-field spectra for heptamer structures with different disk radius *R*. The red line marks the imaging wavelength (λ = 9.3 μm). (c and d) Calculated and experimental near-field amplitude $|E_z|$ and phase φ_z images for the differently sized heptamer structures.

phase image reveals that the central disk is phase-shifted for about only 90° relative to the upper and lower disks. This finding points out the importance of considering both amplitude and phase of the near-field or charge density distribution, in order to fully and unambiguously characterize the oscillation state of the individual metaatoms within complex plasmonic metamolecules.

The phase shift between the central and outer disks at the Fano dip can be explained by considering that the near-field images yield a superposition of the bright mode (all disk dipoles oscillate in phase) and the dark mode (central disk dipole oscillates out of phase with the outer disk dipoles). According to the Alzar model,[36] the dark and the bright modes are phase-shifted for about 90° near the Fano resonance. In the case that the dark mode is dominant—as is the case for small heptamer structures[25]—we expect the central disk dipole being out of phase with the outer disk dipoles for about 180°. However, when the dark and the bright modes have a similar strength—as is the case for our heptamer structure—the phase shift between the central and outer disks is reduced to about 90°. Generally speaking, the phase shift between the central and outer disks can assume any value between 0° and 180° dependent on the individual strengths of the dark and bright modes, which cannot be traced by analyzing only the real part of the charge or near-field distribution.

We note that for any light polarization it is impossible to excite exclusively the dark resonance in symmetric metamolecules, because the dark and bright modes are coupled to each other through the interaction of their optical near fields. To circumvent these limitations, we have performed a second set of experiments with a low-symmetry PI-shaped metamolecule, which is schematically shown in Figure 3a. In this experiment we have used a side-illumination s-SNOM (NeaSNOM, www.neaspec.com, see Figure S1in the Supporting Information), where the sample is illuminated at an angle of around 50° from the surface normal with s-polarized light. Owing to pseudoheterodyne interferometric detection,[35] we are able to record amplitude and phase images at different wavelengths provided by a tunable CO_2 laser. Thus, by tuning the laser frequency across the "dark" resonance, we can observe intensity *toggling* due to Fano interferences in an individual plasmonic metamolecule.

We first experimentally map the near fields of the "dark" (quadrupolar, Q) mode of the PI structure by using horizontally (H-) polarized laser illumination parallel to the short rod (Figure 3c). According to both the calculated reflection spectrum (blue curve in Figure 3b) and near-field distribution (Figure 3c, lower row), the quadrupole resonance occurs at about $\lambda = 10\,\mu$m. The advantage of the H-polarization is that there is no Fano interference with the bright resonance, as confirmed by the Lorentzian profile of the reflectivity spectrum. The near-field amplitude and phase images recorded at λ = 10.2 μm with H-polarization indeed reveal the predicted quadrupole mode structure (Figure 3c, upper row). On both nanorod elements of the PI-structure we find a typical dipole pattern,[30] identified by strong amplitude signals at the rod extremities, which are oscillating out of phase for 180°. What makes the mode "dark" is the opposite alignment of the dipole fields on the two nanorods.

Upon rotation of the sample, i.e., by illuminating the structure with vertical (V-) polarization parallel to the long rods, we track the spatial redistribution of the near fields by tuning the laser frequency across the "dark" resonance. Intensity *toggling* due to Fano interference is demonstrated by near-field imaging at four different wavelengths (marked A−D in the calculated reflection spectrum in Figure 3b). At the spectral position A, we essentially observe the dipole mode of the asymmetric PI structure, while

dx.doi.org/10.1021/nl2021366 |*Nano Lett.* 2011, 11, 3922–3926

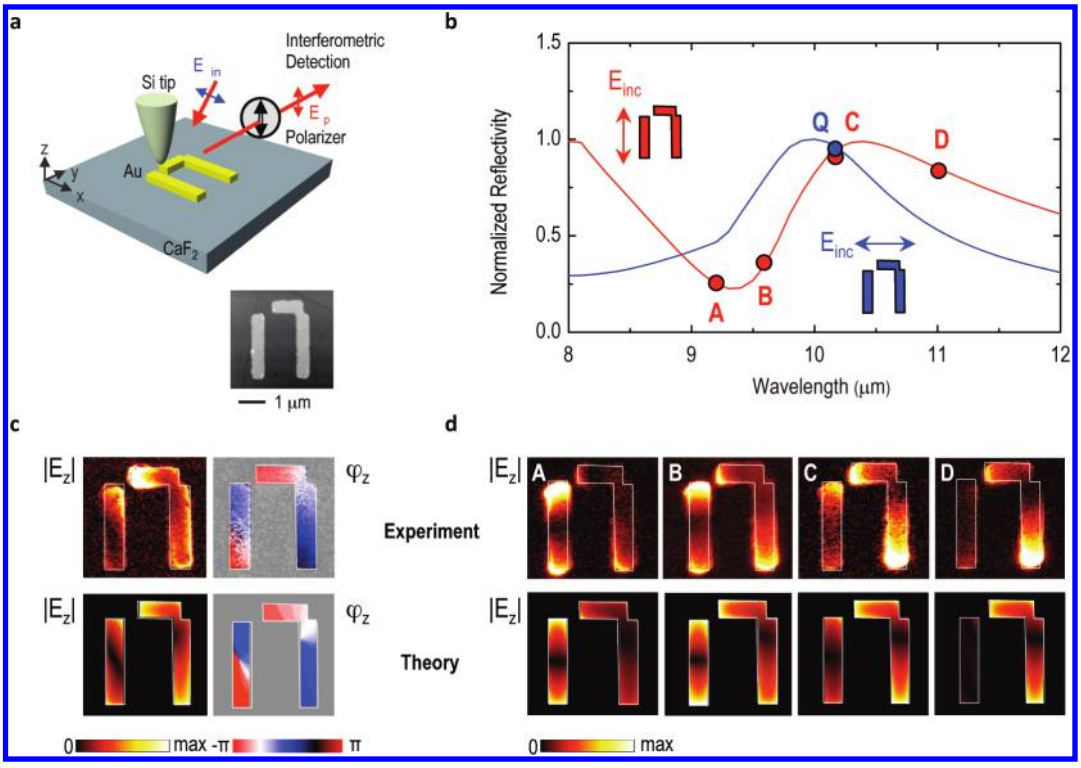

Figure 3. Real-space mapping of Fano interference in asymmetric PI structures. (a) Experimental setup for near-field imaging in reflection mode. The PI structure is illuminated from the side, with s-polarized light. Near-field imaging is performed by recording the tip-scattered radiation with an interferometer, yielding amplitude and phase images simultaneously to topography (gray image below). (b) Numerically calculated reflection spectrum for horizontal (blue) and vertical (red) polarization as indicated by the schematics. The letters mark the spectral positions where near-field imaging was performed. (c) Experimental (upper row) and calculated (lower row) amplitude $|E_z|$ and phase φ_z images for horizontal polarization, recorded at 10.2 μm wavelength. (d) Experimental (upper row) and calculated (lower row) amplitude $|E_z|$ and phase φ_z images for vertical polarization, recorded at the spectral positions A–D marked in (b).

at position C essentially the quadrupolar mode is seen. The constructive/destructive Fano interferences of these two modes are clearly seen by comparing the brightness of the left and right nanorods in images A–D. As the laser wavelength is tuned across the "dark" resonance, the initially bright (image A) left nanorod dims while the initially dark right antenna brightens (image D).

In conclusion, we have used interferometric near-field microscopy to image the interference of "dark" and "bright" modes responsible for Fano resonances in plasmonic metamolecules. The results show dramatic redistributions (*toggling*) of the electric field intensity and phase across the structure as the Fano resonance is traversed and are in excellent agreement with numerical calculations. Real-space near-field imaging provides a fundamental and detailed verification of interfering plasmonic modes and their coupling and thus will be an essential tool for the development of novel spectroscopic applications based on Fano resonances. The insights gained from near-field images will further our understanding of plasmonic Fano resonances and may open up novel applications based on the spectral manipulation of plasmonic near fields.

■ ASSOCIATED CONTENT

Supporting Information. Details of sample fabrication, numerical calculations for PI structures and heptamers, and reflection mode interferometric s-SNOM for mapping plasmon modes. This material is available free of charge via the Internet at http://pubs.acs.org.

■ AUTHOR INFORMATION

Corresponding Author

*E-mail: r.hillenbrand@nanogune.eu, gena@physics.utexas.edu, nordland@rice.edu,

■ ACKNOWLEDGMENT

P.A.-G, M.S., P.S., P.A., and R.H. acknowledge support from the European FP7 project "Nanoantenna" (FP7-HEALTH-F5-2009-241818-NANOANTENNA) and the National Project MAT2009-08393 from the Spanish Ministerio de Ciencia e Innovacion. M.S. and P.S. acknowledges financial support from "Programa de Formación de Personal Investigador" promoted by the Department of Education, Universities and Research of the Basque Government. P.N. and H.S. acknowledge support from the Robert A. Welch foundation (C-1222), the US Department of Defense NSEFF program (N00244-09-1-0067), and the Office of Naval Research (N00244-09-1-0989). C.W., N.A., A. K., and G.S. acknowledge support from the Office of Naval Research (N00014-10-1-0929) and the Air Force Research Laboratory.

■ REFERENCES

(1) Muhlschlegel, P.; Eisler, H. J.; Martin, O. J. F.; Hecht, B.; Pohl, D. W. *Science* **2005**, *308* (5728), 1607–1609.

(2) Curto, A. G.; Volpe, G.; Taminiau, T. H.; Kreuzer, M. P.; Quidant, R.; van Hulst, N. F. *Science* **2010**, *329* (5994), 930–933.

(3) Novotny, L.; van Hulst, N. *Nat. Photonics* **2011**, *5* (2), 83–90.
(4) Chuntonov, L.; Haran, G. *Nano Lett.* **2011**, *11* (6), 2440–2445.
(5) Habteyes, T. G.; Dhuey, S.; Cabrini, S.; Schuck, P. J.; Leone, S. R. *Nano Lett.* **2011**, *11* (4), 1819–1825.
(6) Verellen, N.; Van Dorpe, P.; Huang, C.; Lodewijks, K.; Vandenbosch, G. A. E.; Lagae, L.; Moshchalkov, V. V. *Nano Lett.* **2011**, *11* (2), 391–397.
(7) Zhou, Z.-K.; Peng, X.-N.; Yang, Z.-J.; Zhang, Z.-S.; Li, M.; Su, X.-R.; Zhang, Q.; Shan, X.; Wang, Q.-Q.; Zhang, Z. *Nano Lett.* **2010**, *11* (1), 49–55.
(8) Pryce, I. M.; Aydin, K.; Kelaita, Y. A.; Briggs, R. M.; Atwater, H. A. *Nano Lett.* **2010**, *10* (10), 4222–4227.
(9) Prodan, E.; Radloff, C.; Halas, N. J.; Nordlander, P. *Science* **2003**, *302* (5644), 419–422.
(10) Fedotov, V. A.; Papasimakis, N.; Plum, E.; Bitzer, A.; Walther, M.; Kuo, P.; Tsai, D. P.; Zheludev, N. I. *Phys. Rev. Lett.* **2010**, *104* (22), 223901.
(11) Kao, T. S.; Jenkins, S. D.; Ruostekoski, J.; Zheludev, N. I. *Phys. Rev. Lett.* **2011**, *106* (8), 085501.
(12) Smith, D. R.; Pendry, J. B.; Wiltshire, M. C. K. *Science* **2004**, *305* (5685), 788–792.
(13) Dolling, G.; Enkrich, C.; Wegener, M.; Soukoulis, C. M.; Linden, S. *Science* **2006**, *312* (5775), 892–894.
(14) Liu, N.; Langguth, L.; Weiss, T.; Kastel, J.; Fleischhauer, M.; Pfau, T.; Giessen, H. *Nat. Mater.* **2009**, *8* (9), 758–762.
(15) Papasimakis, N.; Fedotov, V. A.; Zheludev, N. I.; Prosvirnin, S. L. *Phys. Rev. Lett.* **2008**, *101* (25), 253903.
(16) Zhang, S.; Genov, D. A.; Wang, Y.; Liu, M.; Zhang, X. *Phys. Rev. Lett.* **2008**, *101* (4), 047401.
(17) Artar, A.; Yanik, A. A.; Altug, H. *Nano Lett.* **2011**, *11* (4), 1685–1689.
(18) Wu, C.; Khanikaev, A. B.; Shvets, G. *Phys. Rev. Lett.* **2011**, *106* (10), 107403.
(19) Miroshnichenko, A. E.; Flach, S.; Kivshar, Y. S. *Rev. Mod. Phys.* **2010**, *82* (3), 2257.
(20) Fano, U. *Phys. Rev.* **1961**, *124* (6), 1866.
(21) Faist, J.; Capasso, F.; Sirtori, C.; West, K. W.; Pfeiffer, L. N. *Nature* **1997**, *390* (6660), 589–591.
(22) Zhang, W.; Govorov, A. O.; Bryant, G. W. *Phys. Rev. Lett.* **2006**, *97* (14), 146804.
(23) Kroner, M.; Govorov, A. O.; Remi, S.; Biedermann, B.; Seidl, S.; Badolato, A.; Petroff, P. M.; Zhang, W.; Barbour, R.; Gerardot, B. D.; Warburton, R. J.; Karrai, K. *Nature* **2008**, *451* (7176), 311–314.
(24) Fan, J. A.; Bao, K.; Wu, C.; Bao, J.; Bardhan, R.; Halas, N. J.; Manoharan, V. N.; Shvets, G.; Nordlander, P.; Capasso, F. *Nano Lett.* **2010**, *10* (11), 4680–4685.
(25) Fan, J. A.; Wu, C.; Bao, K.; Bao, J.; Bardhan, R.; Halas, N. J.; Manoharan, V. N.; Nordlander, P.; Shvets, G.; Capasso, F. *Science* **2010**, *328* (5982), 1135–1138.
(26) Verellen, N.; Sonnefraud, Y.; Sobhani, H.; Hao, F.; Moshchalkov, V. V.; Dorpe, P. V.; Nordlander, P.; Maier, S. A. *Nano Lett.* **2009**, *9* (4), 1663–1667.
(27) Lassiter, J. B.; Sobhani, H.; Fan, J. A.; Kundu, J.; Capasso, F.; Nordlander, P.; Halas, N. J. *Nano Lett.* **2010**, *10* (8), 3184–3189.
(28) Liu, N.; Weiss, T.; Mesch, M.; Langguth, L.; Eigenthaler, U.; Hirscher, M.; Sönnichsen, C.; Giessen, H. *Nano Lett.* **2009**, *10* (4), 1103–1107.
(29) Hentschel, M.; Saliba, M.; Vogelgesang, R.; Giessen, H.; Alivisatos, A. P.; Liu, N. *Nano Lett.* **2010**, *10* (7), 2721–2726.
(30) Schnell, M.; Garcia-Etxarri, A.; Alkorta, J.; Crozier, K.; Aizpurua, J.; Hillenbrand, R. *Nat. Photonics* **2009**, *3* (5), 287–291.
(31) Schnell, M.; Garcia-Etxarri, A.; Alkorta, J.; Aizpurua, J.; Hillenbrand, R. *Nano Lett.* **2010**, *10* (9), 3524–3528.
(32) Keilmann, F.; Hillenbrand, R. *Philos. Trans. R. Soc., A* **2004**, *362* (1817), 787–805.
(33) Taubner, T.; Korobkin, D.; Urzhumov, Y.; Shvets, G.; Hillenbrand, R. *Science* **2006**, *313* (5793), 1595–1595.
(34) Kim, D.-S.; Heo, J.; Ahn, S.-H.; Han, S. W.; Yun, W. S.; Kim, Z. H. *Nano Lett.* **2009**, *9* (10), 3619–3625.
(35) Ocelic, N.; Huber, A.; Hillenbrand, R. *Appl. Phys. Lett.* **2006**, *89* (10), 101124.
(36) Alzar, C. L. G.; Martinez, M. A. G.; Nussenzveig, P. *Am. J. Phys.* **2002**, *70* (1), 37–41.